Chaotic Hamiltonian ratchets for pulsed periodic double-well potentials: Classical correlations and the ratchet current

N. A. C. Hutchings,[1] M. R. Isherwood,[1] T. Jonckheere,[2] and T. S. Monteiro[1]
[1]*Department of Physics and Astronomy, University College London, Gower Street, London WC1E 6BT, United Kingdom*
[2]*Centre de Physique Théorique, Campus de Luminy case 907, 13288 Marseille cedex 9, France*
(Received 19 December 2003; published 15 September 2004)

We present analytical derivations of the diffusion rates, ratchet currents, and time scales of a new ratchet in a fully chaotic Hamiltonian system, introduced in Phys. Rev. Lett. **89**, 194102 (2002), with a proposed implementation using atoms in pulsed standing waves of light. The origin of this type of ratchet current is in asymmetric momentum diffusion rates which result when a "double-well" lattice is pulsed with unequal "kick" periods. The form of the new short-time correlations which modify the diffusion rates are derived. The resulting formulas for the classical energy diffusion rates are shown to give good agreement with numerical simulations. A closed analytical formula for the ratchet current is also obtained, which predicts correctly the current magnitudes and current reversals. The characteristic "ratchet time," a classical time scale associated with the momentum-diffusion ratchet is derived analytically. The competition between the ratchet time t_r, and the quantum break time t^* is investigated further.

DOI: 10.1103/PhysRevE.70.036205 PACS number(s): 03.65.Sq, 05.45.Mt, 32.60.+i

I. INTRODUCTION

Recent advances in cold atom physics, such as techniques for manipulating atoms in optical lattices, have led to experimental implementation of a rich variety of quantum dynamical phenomena. One particular example is the successful demonstration of dynamical localization [1–3], the so-called quantum suppression of classical chaotic diffusion.

The current interest in coherent atomic dynamics in periodic potentials has been paralleled by burgeoning activity in the area of ratchet dynamics. However, most ratchet studies were motivated by interest in biophysical or mesoscopic systems and involved some form of Brownian motion combined with dissipation [4]. There was little work, in comparison, on Hamiltonian ratchets; the latter are of special significance in cold atom physics since they alone can preserve quantum coherence over longer time scales.

Two exceptions are recent proposals for mixed-phase space ratchets [5,6]. In Ref. [5], the spatiotemporal symmetries which must be broken to generate directed motion were considered. Directed motion was attributed to the desymmetrization of Levy flights. In Ref. [6] a sum rule was obtained for the currents carried by different invariant manifolds in a mixed phase space. From this it was deduced that directed transport in a Hamiltonian system must originate from an inbalance between currents in stable regions (e.g., islands) and currents in the chaotic regions. The fully averaged current for a uniform phase space density of a Hamiltonian system must be zero; this, one can argue, may exclude directed transport in a fully chaotic system [4,6].

In Ref. [7] it was demonstrated that a type of fully chaotic, Hamiltonian directed transport is possible. The proposed system involves broken spatiotemporal symmetries as stipulated in Ref. [5] and does not violate the sum rule since it is unbounded in momentum and therefore does not attain a uniform phase-space distribution. An implementation was proposed using cold atoms in double-well lattices pulsed with unequal periods. The characteristic of this system is an asymmetric diffusion in momentum: in other words, equal numbers of particles would diffuse right or left, say, but one direction would do so with larger momenta, hence generating a net current. Hence we term this a momentum-diffusion ratchet.

A key result of our previous work [7] was to show that there is a distinctive time scale associated with this process: starting from an ensemble of particles with, initially, zero average momentum current $\langle p(t=0)\rangle$, we found the current grows with time. However, eventually, a finite classical current was obtained, with a maximum value reached after a characteristic time scale, the "ratchet time," t_r.

In this system, asymmetry in the momentum distribution accumulates until a finite nonzero value is reached at t_r. While the value of the current saturates to a constant value, the average kinetic energy of the classical ensemble grows without limit. Hence practical implementation of the classical version of the chaotic Hamiltonian ratchet is less interesting. However, for the corresponding quantum system, the phenomenon of dynamical localization "freezes in" this momentum asymmetry, ensuring that the current is not diluted by continual expansion of the momentum distribution. For the maximal quantum current, one must ensure that the quantum break time t^* at which dynamical localization occurs, is approximately the same as the ratchet time t_r, in order to suppress momentum diffusion at the point where the asymmetry is largest.

A related system, an optical lattice with a rocking linear potential, with a similar directed motion mechanism was later investigated by us in Ref. [8]. An experimental version of the latter was demonstrated using cesium atoms in an optical lattice [9]. The double-well ratchet presented here has not yet been investigated experimentally, but is in principle amenable to existing techniques in cold atom physics.

In Ref. [7], only a heuristic derivation of the time scale t_r was presented. While it was explained that the asymmetric

diffusion originates in neglected corrections to the diffusion rate which are obtained when one considers correlations between short sequences of kicks, no expressions were presented. Here we provide formal derivations for t_r and the analytical form to the asymmetric diffusion rate. We also derive a closed analytical expression for the current itself and show that we can predict current reversals without resorting to a numerical study of the dynamics. These are the main new results in this paper.

We show below that the current-generating diffusive correlations of the double-well ratchet are significantly more complicated than for the rocking ratchet in Ref. [8]. For instance, we find that there are in fact several significant time scales corresponding to the different important correction terms. The observed saturation point corresponds simply to the longest one among these.

In Sec. II, we outline the basic features of the physical system. In Sec. III we derive corrections to the diffusion coefficient which give rise to momentum-dependent diffusion rates. We obtain an analytical form for the diffusion coefficient [Eq. (3.9)] that yields close agreement with numerical simulations. We also investigate the time scales involved in the system, and derive the form for t_r [Eqs. (3.12) and (3.13)]. In Sec. IV we obtain a closed formula for the momentum current [Eq. (4.2)] which yields good results and enables us to analyze features of the numerical results such as current reversals. Hence, Eqs. (3.9)–(3.11) and Eq. (4.2) represent the main new equations. In Sec. V we briefly review the quantum behavior of this system and present a few additional results showing the competition between dynamical localization and the classical asymmetric diffusion process. Finally, in Sec. VI, we conclude.

II. THE CHAOTIC HAMILTONIAN RATCHET WITH PULSED DOUBLE-WELLS

The ratchet system introduced in Ref. [7] is based on a modified form of the well-studied Kicked Rotor system, where we have replaced the sinusoidal motion of the rotor with a double well potential

$$V(x) = \sin x + a \sin(2x + \phi) \tag{2.1}$$

and introduced unequally spaced kicks, such that the Hamiltonian for the system becomes

$$H = \frac{p^2}{2} + K[\sin x + a \sin(2x + \phi)] \times \sum_{s=0}^{\infty} \sum_{M=1}^{n\mathrm{cyc}} \delta\left(t - \left(sT_{\mathrm{tot}} + \sum_{i=1}^{M} T_i\right)\right). \tag{2.2}$$

In effect, we have a kicked rotor (the QKR in the quantum case), with a spatially asymmetric potential, kicked with a repeating cycle of unequally spaced "kicks." The T_i are the time intervals between successive kicks, which form a cycle of length $n$cyc, with $T_{\mathrm{tot}} = \sum_{i=1}^{n\mathrm{cyc}} T_i$. This "kicked ratchet" is associated with an effective kicking strength $K_{\mathrm{eff}} = K\sqrt{1+4a^2}$. In the lowest order of approximation, the energy of an ensemble of classical particles grows linearly with time as $\langle p^2/2 \rangle = (K_{\mathrm{eff}}^2/4)t$.

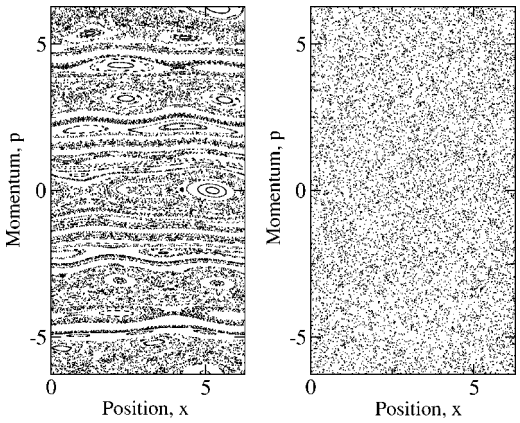

FIG. 1. Poincaré surfaces of section for the chaotic Hamiltonian ratchet. (a) At low kicking strength ($K=0.1$) the asymmetry in the system is already apparent. (b) At $K=2$ the system is in the globally chaotic regime; note the absence of any islands/tori. It is in this regime that our numerical simulations are performed. Each plot was calculated by starting 400 initial trajectories evenly spaced over a range of $x:[0,2\pi]$ and $p:[-10,10]$ then kicking each trajectory 200 times.

The introduction of unequally spaced kicks breaks the time reversal symmetry, which is necessary to generate a nonzero current in the system [7]. In this paper, we focus (as in Ref. [7]) on a cycle of three kicks ($n$cyc$=3$) such that the spacings are $T_1=(1+b)$, $T_2=1$ and $T_3=(1-b)$, with b a small parameter.

For low values of the kicking strength K, the classical phase space demonstrates the momentum asymmetry in the dynamics, with islands and tori having no partners at corresponding negative momenta. A key feature of our system is that it works in the regime of global chaos and does not depend on the presence of regular structures in phase space. A typical Poincaré surface of section from the parameter space we have studied is shown in Fig. 1, showing the absence of visible islands or KAM tori.

The observed build up, with time, of asymmetry in the momentum distribution is due to differing classical momentum diffusion rates for particles with positive momenta relative to those with negative momenta. For physical insight (and before we derive a more rigorous treatment of the diffusion process in the next section), we show in Fig. 2 the energy absorbed by an ensemble of particles for a typical set of parameters. At $t=0$ all the particles had $p=0$. We plot separately the total energy of the particles with negative momenta and those with positive momenta, as a function of time. The figure shows clearly that for $b=0.05$, and time $t<2000$ or so, particles with positive momenta absorb kinetic energy significantly more slowly than particles with negative momenta. But the average is close to the well known "quasilinear" rate $\langle E \rangle = D_{\mathrm{ql}} t = (K_{\mathrm{eff}}^2/4)t$, associated with a random walk in momentum space. These rates appear to equalize after a certain time and to revert to $D \simeq D_{\mathrm{ql}}$.

From Fig. 2 one can clearly see that the energy splitting is not only momentum dependent, but that the corresponding ratchet time is dependent on b, the perturbation to the kicking period. In Ref. [7] we attributed the cause of these dif-

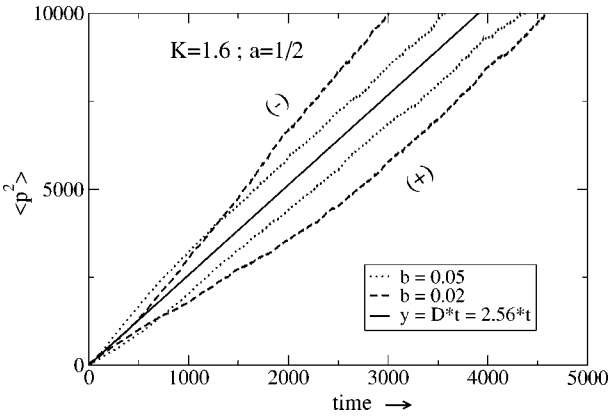

FIG. 2. Figure illustrates differential energy absorption for particles with positive and negative momenta. An ensemble of particles (all with $p=0$ at initial time, $K=1.6$, $a=0.5$) is evolved, and $\langle p^2\rangle$ is calculated separately, at each time, for particles with positive and negative momenta. The two upper curves [near the $(-)$ sign] show $\langle p^2\rangle$ as a function of time for particles with negative momentum and two different values of b, the two lower curves [near the $(+)$ sign] show the corresponding curves for particles with positive momentum. We see that particles with negative momenta, for a certain time period absorb energy faster than those with negative momenta. Note also that the behavior becomes linear after a certain time.

fering diffusion rates to correlations between short sequences of kicks in the evolution sequence, yielding corrections to overall diffusion rate. In effect, the diffusion rate for this system becomes local in momentum $D\equiv D(p,t)$. It is also not linear in time — as seen below, except for very short times and for very long times. In the next section we derive in detail these corrections, investigate the time scales involved and hence can analyze the general behavior seen in Fig. 2.

III. THE MOMENTUM DIFFUSION COEFFICIENT

At the lowest level of approximation in ratchet and rotor systems, the growth of the average energy, in the absence of phase space barriers, can be approximated by the quasilinear formula $D_{\rm ql}\approx K^2/4$ [10]. However, this approximation neglects the effect of correlations between consecutive kicks which can significantly modify the diffusion coefficient. In the case of the standard map [corresponding, in Eq. (2.2) to $a=0, b=0$], the energy growth for an ensemble of classical particles with initial momentum p_0 is given by

$$\left\langle \frac{(p-p_0)^2}{2} \right\rangle = Dt \equiv D_0 t + t\sum_{l=1}^{\infty} C(l,p), \tag{3.1}$$

where the $C(l)$ terms are corrections to the quasilinear diffusion resulting from correlations between successive kicks.

These corrections have been studied extensively for the standard map, resulting in an adjusted diffusion coefficient [10,11]:

$$D = \frac{K^2}{4}\{1 - 2[J_1(K)]^2 - 2J_2(K)\cdots\}. \tag{3.2}$$

Here, for example, the $-J_2(K)$ term arises from the two-kick correlation which has the form $C(2,p)=\langle V'(x_i)V'(x_{i+2})\rangle$. Here x_i is the x coordinate after kick i and the average is carried out over all phase-space coordinates. One can clearly see that for the standard map, the diffusion coefficient is momentum independent. As the results below show, in our case, the diffusion coefficient becomes momentum dependent. The calculation, outlined below, is an extension of the method of Rechester and White [12], and is detailed in full in the Appendix.

Starting with an initial momentum p_0, the diffusion coefficient can be written in terms of the conditional probability density Q that the system evolves to a state (x_N,p_N) at time $t=N$ (that is, after N kicks):

$$D(N) = \frac{1}{2N}\int Q(x_N,p_N,N|x,p,0)P(x,p,0) \times (p_N-p)^2 dx_N dp_N dx dp, \tag{3.3}$$

where the initial probability distribution is given by

$$P(x,p,0) = (2\pi)^{-1}\delta(p-p_0).$$

Using the recursion property of the conditional probability Q, and the 2π periodicity in the x variable, we can write the diffusion coefficient as (see the Appendix):

$$D = \lim_{N\to\infty}\frac{1}{2N}\sum_{m_N=-\infty}^{\infty}\cdots\sum_{m_1=-\infty}^{\infty}\prod_{i=0}^{N}\int_0^{2\pi}\frac{dx_i}{(2\pi)}S_N^2 \times \exp\left(\sum_{j=1}^{N}\{\mathrm{im}_j[x_j - x_{j-1} - (t_j - t_{j-1})(p_0+S_{j-1})]\}\right), \tag{3.4}$$

where we define

$$S_j = -\sum_{l=0}^{j} V'(x_l). \tag{3.5}$$

By setting $\mathrm{m}_j=0$ for all j in the above formula, one simply recovers the quasilinear diffusion. In order to examine the contribution of various correlations one must look at the product of terms where the m_j are set to an appropriate nonzero value.

The main corrections to the diffusion rate for the ratchet are found by considering the two-kick correlations $C(2,p)$, i.e., choosing the term $2V'(x_i)V'(x_{i+2})$ in the product $S_N^2 = S_N S_N$. For small b, the leading contribution to this correction comes by taking $m_{i+2}=\pm 1$ and $m_{i+1}=-m_{i+2}$ (all other m_j zero; this gives the contribution of the $K\sin x$ part of the potential), or $m_{i+2}=\pm 2$ and $m_{i+1}=-m_{i+2}$ (contribution of the $\sin 2x$ part of the potential). Since there are three different time intervals possible between kicks i and $i+2$ (T_1+T_2, or T_2+T_3, or T_3+T_1), one has to calculate three different contributions for these three cases. Summing the results for all

kicks i between 1 and N, we get a contribution from the $\sin x$ part of the potential (the full derivation is contained in the Appendix):

$$C_{\sin x}(2,p) = -\frac{K^2}{6}\Bigg[\sum_{-\infty}^{\infty} J_{2-2s}(K(1+b))J_s(2Ka(1+b)) \times\cos\left(2p_0b+\frac{\pi}{2}s\right) + \sum_{-\infty}^{\infty} J_{2-2s}(K)J_s(2Ka) \times\cos\left(p_0b-\frac{\pi}{2}s\right) + \sum_{-\infty}^{\infty} J_{2-2s}(K(1-b)) \times J_s(2Ka(1-b))\cos\left(p_0b-\frac{\pi}{2}s\right)\Bigg]. \quad (3.6)$$

The sum over s formally spans the range $s=\pm\infty$, but for typical K values converges for $|s|<20$. This result is valid for short times. For longer times (that is, larger kick value N), the correction to the average energy growth is no longer linear in time, and eventually saturates to a given value. This is discussed later, together with the ratchet time.

The cosines in Eq. (3.6) can be expanded; for example, the first term in Eq. (3.6) becomes

$$C^{(1)}_{\sin x} = \frac{K^2}{6}\sum_s J_{2-2s}(K(1+b))J_s(2Ka(1+b)) \times\left(\cos 2p_0b\cos\frac{\pi}{2}s - \sin 2p_0b\sin\frac{\pi}{2}s\right).$$

If we wish to consider only the build up of asymmetry in the system about $p=0$, we can neglect the even terms. The asymmetry which drives the directed transport is due solely to the $\sin np_0b$ ($n=1, 2, 4$) dependent terms in the diffusion coefficient (those which are odd with respect to reflection about $p=0$). We therefore simplify Eq. (3.6) to

$$C^{(\mathrm{asymm})}_{\sin x}(2,p) = \frac{K^2}{6}\Bigg[\sum_s J_{2-2s}(K(1+b))J_s(2Ka(1+b)) \times\sin 2p_0b\sin\frac{\pi}{2}s - \sum_s J_{2-2s}(K)J_s(2Ka) \times\sin p_0b\sin\frac{\pi}{2}s - \sum_s J_{2-2s}(K(1-b)) \times J_s(2Ka(1-b))\sin p_0b\sin\frac{\pi}{2}s\Bigg]. \quad (3.7)$$

A similar equation is obtained for the $Ka\sin 2x$ part of the ratchet potential

$$C^{(\mathrm{asymm})}_{\sin 2x}(2,p) = \frac{(2Ka)^2}{6}\Bigg[-\sum_s J_{4-2s}(2K(1+b))J_s(4Ka(1+b)) \times\sin 4p_0b\sin\frac{\pi}{2}s + \sum_s J_{4-2s}(2K)J_s(4Ka) \times\sin 2p_0b\sin\frac{\pi}{2}s + \sum_s J_{4-2s}(2K(1-b)) \times J_s(4Ka(1-b))\sin 2p_0b\sin\frac{\pi}{2}s\Bigg]. \quad (3.8)$$

These formulas can now be rearranged to give the total correction to the diffusion coefficient as a function of the three $\sin npb$ present (note that we use $s'=2-2s$ and $s''=4-2s$ for clarity):

$$C^{(\mathrm{asymm})}(2,p) = -\frac{K^2}{6}\Bigg[\sin p_0b\Bigg\{\sum_s [J_{s'}(K)J_s(2Ka) + J_{s'}(K(1-b))J_s(2Ka(1-b))]\sin\frac{\pi}{2}s\Bigg\} - \sin 2p_0b\Bigg\{(2a)^2\sum_s [J_{s''}(2K)J_s(4Ka) + J_{s'}(K(1+b))J_s(2Ka(1+b)) + (2a)^2 \times J_{s''}(2K(1-b))J_s(4Ka(1-b))]\sin\frac{\pi}{2}s\Bigg\} + \sin 4p_0b\Bigg\{(2a)^2\sum_s J_{s''}(2K(1+b)) \times J_s(4Ka(1+b))\sin\frac{\pi}{2}s\Bigg\}\Bigg]. \quad (3.9)$$

The form above does not incude the time dependence or information on the ratchet time scales. An analytical form for these time scales is obtained by taking the full time dependence into account in the calculations (see the Appendix). For each $\sin np_0b$ term, there is a time-dependent function $\Phi(N,bK,n)$. We rewrite Eq. (3.9) as a Fourier series, with the Bessel function products replaced by coefficients A_n:

$$C^{(\mathrm{asymm})}(2,p) = -\frac{K^2}{6}\left[A_1\sin p_0b - A_2\sin 2p_0b + A_4\sin 4p_0b\right]. \quad (3.10)$$

The Bessel sum can easily be evaluated: for example, for $K=14$, $a=1/2$, $b=0.005$, we find $A_1=0.13$ so the $\sin p_0b$ term is weighted by a coefficient $(K^2/6)A_1=4.3$, which will later be compared to numerical values.

To go beyond the form valid only at short times, we must weight each term by $\Phi(N,bK,n)$, where N is the number of kicks and $N=t$. Hence,

$$C^{(\mathrm{asymm})}(2,p) = -\frac{K^2}{6}\big[A_1\Phi(N,bK,1)\sin p_0 b - A_2\Phi(N,bK,2)\sin 2p_0 b + A_4\Phi(N,bK,4)\sin 4p_0 b\big]. \quad (3.11)$$

The leading term is the time-behavior function $\Phi(N,bK,1)$, which can be shown to take the form (see the Appendix)

$$\Phi(N,bK,1) = \frac{3}{N}\frac{1-[J_0(bK)J_0(2abK)]^{N-1}}{1-[J_0(bK)J_0(2abK)]^3} \quad (3.12)$$

[to obtain the form for $\Phi(N,bK,2)$ we would simply double the arguments of the Bessel functions above and for $\Phi(N,bK,4)$ we would quadruple them].

For small b and small N, $\Phi(N,bK,n)\simeq 1$, which leads to the linear correction to the energy: in this regime we could write $\langle (p-p_0)^2/2\rangle \simeq Dt \equiv D_0 t + C(2,p)t$ as in Eq. (3.1). We recall that $C(2,p)=C^{(\mathrm{asymm})}(2,p)+C^{(\mathrm{symm})}(2,p)$ and only the $C^{(\mathrm{asymm})}(2,p)$ term represents diffusion asymmetric about $p=0$ and hence the ratchet effect.

However, for larger N, eventually $\Phi(N,bK)\sim 1/N$ so the contribution of the two-kick correction $C^{(\mathrm{asymm})}\times(2,p)\Phi(N,bK)t$ tends to saturate to a constant value. The saturation time for the leading term $\Phi(N,bK,1)$ (which is the most long lived) is the ratchet time.

The ratchet time can be estimated by finding the time at which $\Phi(N,bK,n=1)t$ reaches 95% of its value at $N=\infty$. This is found to be, for $a=1/2$:

$$t_r^{(\sin pb)} = \frac{2\ln(20)}{(Kb)^2} \approx \frac{6}{(Kb)^2}. \quad (3.13)$$

The heuristic arguments in Ref. [7] gave a time scale $t_r \sim 2\pi/(Kb)^2$ which is not too different. The same analysis can now be repeated to obtain the separate (shorter) time scales corresponding to the $\sin 2pb, \sin 4pb$ corrections. It is straightforward to show that $4t_r^{(\sin 2pb)} \simeq t_r^{(\sin pb)}$ and $16t_r^{(\sin 2pb)} \simeq t_r^{(\sin pb)}$.

Note that for large N, $\Phi(N)t$ saturates to the value of $\sim 1/[(bK)^2]$. The energy growth is no longer affected by the two-kick correlations and contains no asymmetric diffusion component. This results in a progressive dilution of the asymmetry in the classical case (but not the quantum case). One also notes that the ratchet effect is clearly dominated by the time scale corresponding to the $\sin pb$ term (the two other ratchet times are, respectively, $1/4$ and $1/16$ smaller).

Figure 3(a) plots $\langle (p-p_0)^2\rangle = E(p_0, N=100)$, the average kinetic energy, after $N=100$ kicks, of an ensemble of 10^6 particles (which all had $p=p_0$ at $N=0$). These numerics enable us to obtain numerical estimates of the coefficients $(K^2/6)A_n$. Now at short times, $E(p_0,N)\simeq D_0 t + C(2,p)t$ and includes both the symmetric and asymmetric terms in the diffusion coefficient. In Figs. 3(b) and 3(c) we have removed the symmetric contribution (and $D_0 t$) by plotting $E(N)_{\mathrm{asymm}} = \frac{1}{2}[E(p_0,N)-E(-p_0,N)]$. Figure 3(b) shows $E_{\mathrm{asymm}}(p_0, N=20)$, whereas Fig. 3(c) shows $E_{\mathrm{asymm}}(p_0, N=100)$. We can now fit a Fourier series in $\sin p_0 b$ to each curve and obtain

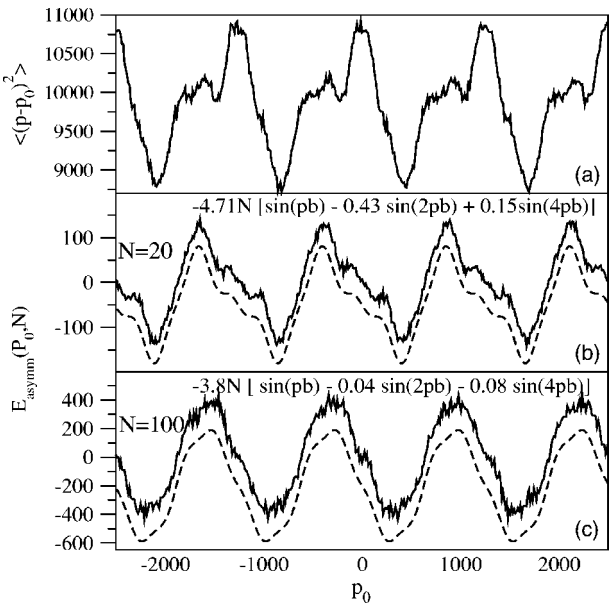

FIG. 3. (a) Average classical kinetic energy $E(p_0, N=100)$ plotted as a function of initial momentum p_0, calculated numerically for an ensemble of 10^6 particles with $K=14$, $a=1/2$, $b=0.005$ time $t=100$. In (b) and (c) we have removed the momentum-independent and symmetrical $\cos npb$ contributions by plotting $E_{\mathrm{asymm}}(P_0,N) = \frac{1}{2}[E(p_0,N)-E(-p_0,N)]$. The energy spread after 20 kicks is shown in (b) and after 100 kicks in (c). The dashed curves, are obtained by Fourier analysis of the numerical results. For clarity, these curves have been shifted vertically.

the relative amplitudes for each of the three terms that appear in our analytical formula (3.9); $\sin p_0 b, \sin 2p_0 b$, and $\sin 4p_0 b$. The Fourier coefficients are indicated in the figure. One can clearly see that for the example given, the relative amplitudes of the terms vary with time: at 20 kicks there is a strong contribution from the $\sin 2pb$ term, whereas after 100 kicks the $\sin 2pb$ contribution is an order of magnitude smaller and the curve is almost a pure $\sin pb$. The $\sin pb$ weighting coefficients estimated from the graphs, 4.7 and 3.8 compare favorably with the estimate of Eq. (3.10), where we calculate $(K^2/6)A_1 = 4.3$.

Figure 4 shows the dependence of the amplitudes of each of the sine terms on kick strength K after 20, 40, and 100 kicks. Also shown is the analytical form for each term as predicted in Eq. (3.9). It can be clearly seen that the $\sin pb$ contribution persists beyond 100 kicks for all values of K. The $\sin 2pb$ contribution is still significant at 40 kicks for all values of K, but has been significantly damped by 100 kicks for $K>10$. The time scale over which the $\sin 4pb$ contribution is appreciable is shorter still. For $K>6$ the amplitude at 100 kicks is virtually negligible while at 20 and 40 kicks it is heavily damped.

In Fig. 5 the ratchet time is plotted against the parameters b and K. Each point on the graph corresponds to a measurement of t_r for a given parameter set. The value of t_r was estimated by taking a running average over 50 kicks and measuring the standard deviation in $\langle p\rangle$ of the ensemble of 400000 trajectories. When the deviation fell to below 5% of the maximum the value of t_r was assigned. In Fig. 5(a) the

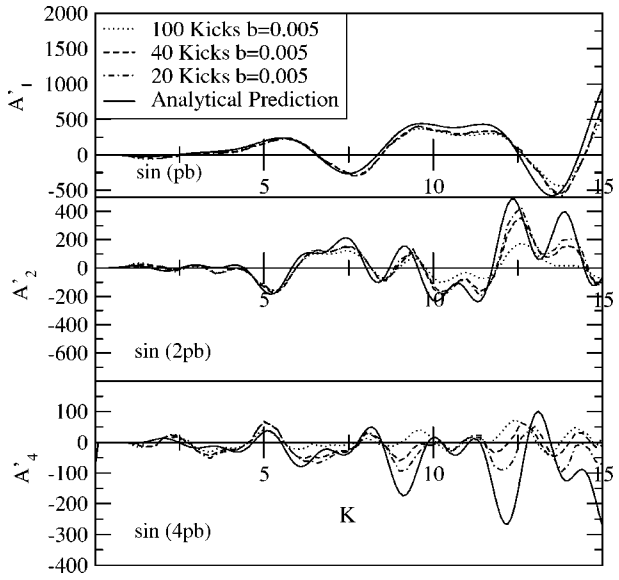

FIG. 4. Contributions to classical asymmetric energy diffusion that arise from $\sin(npb)$ terms in the first order correction to the diffusion constant are shown as a function of K. Analytically predicted amplitudes are compared with numerical results for varying numbers of kicks to highlight the time scales involved. The amplitudes are scaled to 100 kicks for comparison, i.e., $A_n' = A_n(K^2/6)(100/N)$. One can see in (a) that the numerical results for the $\sin(pb)$ term show excellent agreement with the analytical prediction for all K, suggesting that this term continues to influence the final current past 100 kicks. In (b) one sees good agreement for both 20 kicks and 40 kicks up to fairly high K, whereas after approximately $K=10$ the 100 kick curve begins to depart markedly from the analytical prediction. This suggests that for high kick strength the contribution to the final current from the $\sin(2pb)$ term has been damped by 100 kicks. This effect is even more noticeable for $\sin(4pb)$ as shown in (c). Good agreement between numerics and analytics exists only up to approximately $K=5$ with the 100 kick curve becoming heavily damped soon after. One can clearly see the 40 kick curve departing from the analytical result more quickly and completely than the 20 kick result. These plots show that for increasing kick strength, the time scale over which each term contributes to the final current changes.

value of b is varied across a wide range while the kicking strength K is kept constant. The plot shows clear numerical evidence of the $1/b^2$ proportionality of the ratchet time. A fit of $t_r = 2\pi/(Kb)^2$ is plotted against the numerical results and very good agreement can be seen. In the lower panel [Fig. 5(b)] the parameters are exchanged and K^2 is varied against a constant b. Once again the numerical results bear out an excellent correspondence to the expected $t_r \simeq 6/(Kb)^2$ relationship obtained from the $\sin pb$ term above.

IV. THE RATCHET CURRENT

It is possible to obtain an analytical form for the classical ratchet current shown in Fig. 7, using a very similar method to that used to obtain the diffusion coefficient. In this case we define the average current at a given time to be

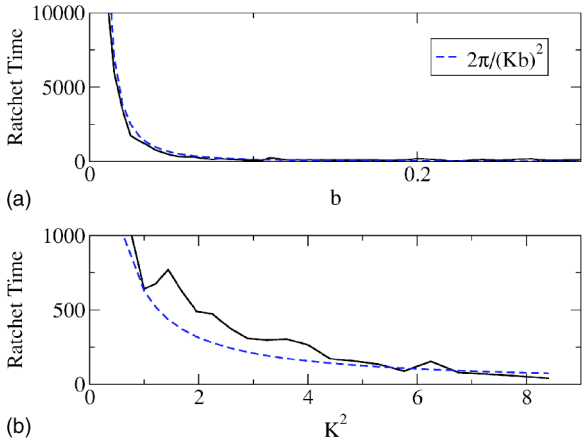

FIG. 5. Classical ratchet saturation time, measured in kicks, versus system parameters b (a) and K^2 (b). (a) The classical ratchet time is measured when the deviation of a 100 kick running average falls below 2% of its maximum value. A very good numerical agreement (solid line) is shown to a fit of $2\pi/K^2b^2$ (dashed line). The value of K was fixed at 1.6. (b) using the same measurement technique for (a) the ratchet time is plotted against K^2 for a fixed $b=0.1$. Again a nonlinear curve fit of $2\pi/K^2b^2$, (dashed line) is compared to the numerical results (solid line). Each point on each graph is a result of a classical calculation of 500 000 trajectories run over 10 000 kicks.

$$\langle p(N)\rangle = \int Q(x_N,p_N,N|x_0,p_0,0)P(x_0,p_0,0)(p_N-p_0)dx_N dp_N. \tag{4.1}$$

It is easily shown that, similar to the asymmetric energy diffusion, the momentum current increases with N and then saturates after a time scale $t_r \sim 1/(Kb)^2$. This is unsurprising, since the two share a common physical origin.

We evaluate the saturated current, $\langle p(N\to\infty)\rangle$. The leading order term for the average saturated current obtained using the modified Rechester and White approach is then

$$\begin{aligned}\langle p(N\to\infty)\rangle = {} & K\frac{J_1(bK)J_0(2abK)}{1-[J_0(bK)J_0(2abK)]^3} \\ & \times\sum_s \sin\left(p_0 b-\frac{\pi}{2}s\right)J_{2-2s}(K)J_s(2aK) \\ & -2Ka\frac{J_0(2bK)J_1(4abK)}{1-[J_0(2bK)J_0(4abK)]^3} \\ & \times\sum_s \sin\left(p_0 b-\frac{\pi}{2}s\right)J_{4-2s}(2K)J_s(4aK), \end{aligned} \tag{4.2}$$

where the approximation $1-b\approx 1$ has been made. The first term in Eq. (4.2) arises from the $K\sin x$ part of the potential, and the second term is the contribution from $Ka\sin 2x$.

We note that the momentum current tends to a constant value as $t\to\infty$. However the width of the momentum distribution continues to grow as $D_0 t$. Hence the momentum current, normalized to the width of the momentum distribution,

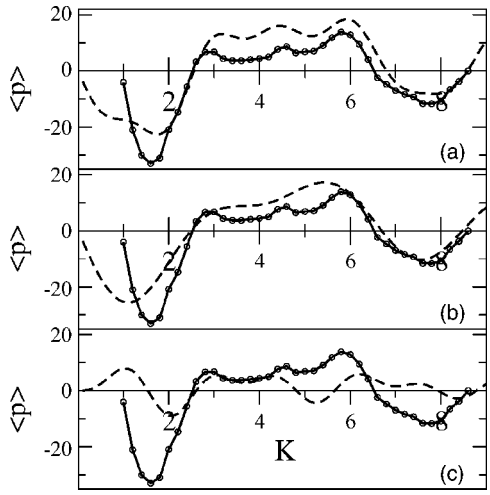

FIG. 6. Comparison of numerical and analytical average current as a function of kicking strength K. In (a) the leading order analytical term (dashed line) given by Eq. (4.2) is shown with the numerical result (circles) for $b=0.01$ and $a=1/2$. Note that the current reversals are accurately predicted, as is the general trend of the numerical curve. Panel (b) shows the contribution from the first term in Eq. (4.2), due to the $\sin x$ part of the potential. The final panel (c) shows the contribution from the second term, due to $\sin 2x$. Both curves are plotted with the numerical result.

will tend to zero in the classical case, but—as discussed in the next section—will tend to a constant in the quantum case.

The top panel of Fig. 6 shows a comparison of this result with numerical simulation for $b=0.01, a=0.5$, and zero initial momentum. The individual contributions from each term in Eq. (4.2) are shown in the lower two panels of the figure. The shape of the curve is clearly dominated by the $K\sin x$ part of the potential, but one can easily see where the $Ka\sin 2x$ part competes, for example, to create the dips between $K=3\rightarrow 6$. While the current reversals are accurately predicted and the general trend of the curve is in keeping with the numerical results, there are some features which are not in keeping with expectation. In the region $0\leqslant K\leqslant 2$ the numerical current appears to decrease much more rapidly than the analytical prediction. This is possibly due to the increasing regularity of the system inhibiting the build up of asymmetry. Once beyond the current reversal at $K=2.6$, the magnitude of the current never reaches that of the analytical curve. In this region the ratchet time is short, and the asymmetry in the system is washed out by the expansion of the classical momentum distribution. Also, Eq. (4.2) is the leading order term for the current, resulting from the second order correlations. One would expect that including higher order terms might well affect the predicted current, and improve the accuracy of the result. Furthermore, the analytical form is valid in the regime of small b, and one would anticipate that the numerical curve will tend to the theoretical prediction as $b\rightarrow 0$. A fuller numerical investigation of the dependence on b and a is given in Ref. [13].

V. COMPETITION BETWEEN t_r AND t^*

Having considered exclusively the *classical* diffusion mechanism underpinning this ratchet in the previous sections, we must now examine the corresponding *quantum* behavior. The implementation of this type of ratchet is best done using cold atoms in optical lattices, a system far from the classical limit. Here we review in brief the quantum results obtained in Ref. [7] and extend those calculations to test a wider parameter range.

In the quantum case, in addition to the dynamical parameters K,a,b we must consider $\hbar$ (note that in the experiment, a rescaling of coordinates introduces an effective value of $\hbar$. In a typical experiment $\hbar\sim 0.25-2$). A conclusion of Ref. [7] was that the key to achieving the most distinctive experimental asymmetry lies in approximately equalizing the two time scales of the system: the classical ratchet time t_r and the quantum break time t^*. We recall that for the standard quantum kicked rotor (QKR), $t^*\sim D/\hbar^2$. In our case we still have a time-periodic system (though with a time period in effect three times longer than the QKR) so its time evolution can be determined by an expansion over the underlying Floquet states: in the long-time limit its behavior is quasiperiodic and diffusion is suppressed as in the QKR.

A numerical study in Ref. [7] found that dynamical localization proceeds in a similar way to the QKR. For each particular set of dynamical parameters K, a, b, and $\hbar$, the time evolution of a minimal uncertainty wave packet was calculated in a plane-wave basis. A quantum probability distribution for the momentum $N(p,t)$ was obtained as a function of time. From this it is simple to compute the expectation values of the momentum $\langle p\rangle$, the energy $\langle p^2\rangle$ as well as the saturation time for the energy t^*. In our system, unlike the QKR, we have a local (in momentum) diffusion rate $D(p)$ which oscillates with momentum (with period $2\pi/b$, see Fig. 3) about the uncorrelated value $D_0=K_{\mathrm{eff}}^2/4$. For the parameters considered here, the amplitude of these oscillations is not large compared with D_0. In that case, we found from numerics in Ref. [7] that the break time corresponds closely to the averaged value $t^*\sim 20(D_0/\hbar^2)$ [13].

It is interesting to contrast this with the rocking lattice system and experiment in Refs. [8,9] which corresponded to the opposite limit: if the amplitude oscillations in the two-kick correlations are large relative to the uncorrelated rate D_0, and $b\sim 0.01$ is small, the typical width of $N(p)$ is small relative to $2\pi/b$. For a narrow momentum distribution $N(p_0-p)$, strongly peaked about a momentum $p=p_0$, one needs to consider a local break-time $t(p_0)^*\sim D(p_0)/\hbar^2$ which can vary by a factor of ~ 100 as one varies the initial drift momentum p_0 of the atoms relative to the optical lattice [8]. However, this is not the situation here. For this system we find that $t^*\simeq 20(K_{\mathrm{eff}}^2/\hbar^2)$ represents a good approximation, for all values of b.

If the quantum diffusion persists as long as t_r, the quantum system acquires the full classical asymmetry. Hence the condition $t^*\sim t_r$ ensures that the maximal classical asymmetry is frozen in and that the asymmetry is not diluted by the continual spread of the classical momentum distribution. Evidence for this criterion is shown in Fig. 7, where the classical and quantum currents (after saturation) are shown for various parameter choices. For the quantum case, $\hbar$ is decreased from $\hbar=1/2$ to $\hbar=1/8$ while keeping b, the perturbation to the period, constant at $b=0.1$. For the lower

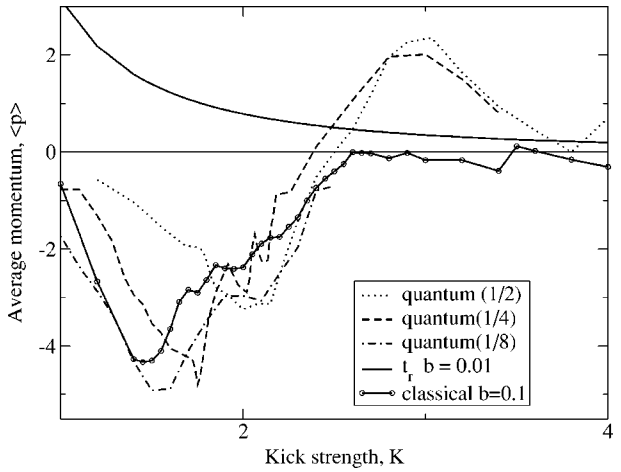

FIG. 7. Variation of average classical and quantum currents as a function of kick strength K. Numerical values in brackets indicate the value of $\hbar$. In the quantum case, where $b=0.1$ for each curve, one notes that there is an improving fit with the classical $b=0.1$ curve for decreasing $\hbar$. At low K the break time for $\hbar=0.5$, 0.25 is too short, and the system localizes before the maximum amount of classical asymmetry has been reached. As K is increased, t^* increases and the classical and quantum plots show good agreement once $t^* \approx t_r$. While both the quantum and classical curves share the same crossing, the classical curve for $b=0.1$ does not show the positive peak that features in both quantum graphs. This is due to the fact that the ratchet time is now too short to allow any appreciable build up of classical asymmetry (shown by the scaled ratchet time curve). The classical peak is recovered at smaller b (not shown), and therefore increasing t_r for a given value of K.

values of the kicking strength $K \sim 2.5$ or less, one can see that the quantum current approaches the classical current for $b=0.1$ as $\hbar$ is decreased. Recalling that $t^* \propto 1/\hbar^2$ we see the effect of the changing break times: in the range $K=2-2.5$ all the curves ($\hbar=1/2, 1/4, 1/8$, and classical) are roughly in agreement. In this range all values of $\hbar$ allow time for asymmetry to accumulate. However, for $K=1.5-2$, for $\hbar=1/2$ and $1/4$, in this range, $t^* < t_r$ so the quantum current falls below the classical value. The quantum momentum distribution localizes before the full asymmetry is achieved. However, $\hbar=1/8$ follows quite closely the classical behavior in this range since it has a break time 16 times longer than for $\hbar=1/2$.

As the kick strength is increased beyond the crossing (approximately $K \approx 2.6$) one notes that there is once again a large discrepancy between the classical and quantum results. The ratchet time decreases with increasing K (as shown by the scaled t_r curve shown in the figure), and when the ratchet time is too short, the calculated classical asymmetry is negligible. Perhaps surprisingly though, the corresponding quantum system still exhibits significant asymmetry. In fact the quantum behavior corresponds more closely to the classical current for somewhat smaller values of $b<0.1$: when t_r is very small we get poor agreement between classical and quantal results, even with small $\hbar$. It is clear that some details of the quantum classical correspondence here will only be understood from a detailed study of the properties of the Floquet states of this quantum system, which is currently underway.

By decreasing the parameter b (and therefore increasing t_r) the classical current for high K once again approaches the quantum current. In broad terms however, we conclude that while the basic ratchet mechanism is a classical one, the best experimental results will be obtained with $t^* \sim t_r$. The best quantum-classical agreement will be obtained in the parameter ranges where neither t^* nor t_r are too small.

VI. CONCLUSION

We have derived analytical expressions for the energy diffusion rates, the classical ratchet currents, and the ratchet time. We have shown that we can fully characterize the behavior of the only chaotic Hamiltonian ratchet mechanism proposed to date. This new type of Hamiltonian ratchet is in fact a momentum-diffusion ratchet. The current is generated by differential acquisition of kinetic energy by particles moving right or left, rather than an asymmetry in the global numbers of particles moving right or left. Finally we have analyzed the corresponding quantum behavior. We have demonstrated the importance of an appropriate choice of ratchet time and quantum break time in obtaining the best experimental momentum asymmetries.

ACKNOWLEDGMENTS

The authors acknowledge support from the EPSRC.

APPENDIX: DERIVATION OF CORRECTION TERMS

In order to obtain the diffusion coefficient for the ratchet we begin by defining the generalized map

$$x_{j+1} = x_j + p_{j+1}(t_{j+1} - t_j), \tag{A1}$$

$$p_{j+1} = p_j - V'(x_j), \tag{A2}$$

where $t_{j+1} - t_j$ is the time between successive kicks $j+1$ and j. For the standard map, these intervals are the same for all kicks. However, this is not true for our chirped sequence. As explained in the text, we consider explicitly a cycle of three different intervals $(1+b)$, 1 and $(1-b)$, with b a small parameter. From the map we have

$$p_N = p_0 - V'(x_0) - V'(x_1) \cdots - V'(x_{N-1}) = p_0 - \sum_{l=0}^{N-1} V'(x_l)$$

and so we define

$$S_j = -\sum_{l=0}^{j} V'(x_l). \tag{A3}$$

We use the standard definition of the diffusion coefficient

$$\left\langle \frac{(p-p_0)^2}{2} \right\rangle = D(t)t \tag{A4}$$

and assume that the systems starts at $p=p_0$ at time $t=0$. If we consider the diffusion in terms of the conditional probability density Q that the system evolves from the state (x

$\in[0,2\pi], p=p_0)$ at time $t=0$ to the state $(x=x_N, p=p_N)$ at time $t=t_N$ we find

$$D(t_N) = \frac{1}{2t_N}\int Q(x_N,p_N,t_N|x,p,0)P(x,p,0) \times (p_N-p)^2 dx_N dp_N dx dp, \tag{A5}$$

where the initial probability distribution is given to be

$$P(x,p,0) = (2\pi)^{-1}\delta(p-p_0)$$

and Q obeys the recursion property

$$Q(x_N,p_N,t_N|x_0,p_0,0) = \int Q(x_N,p_N,t_N|x_i,p_i,t_i) \times Q(x_i,p_i,t_i|x_0,p_0,0)dx_i dp_i. \tag{A6}$$

Inserting this property successively for each kick between N and 0 in Eq. (A6), and using

$$Q(x_N,p_N,t_N|x_{N-1},p_{N-1},t_{N-1}) = \sum_{n_N=-\infty}^{+\infty}\delta(p_N-p_{N-1}+KV'(x_{N-1})) \times \delta(x_N-x_{N-1}-(t_N-t_{N-1})[p_{N-1} - KV'(x_{N-1})]+2\pi n_N) \tag{A7}$$

where the sum over n_N occurs because of the periodic boundary condition for x_N $(0\leqslant x_N\leqslant 2\pi)$, we obtain

$$\begin{aligned} Q(x_N,p_N,t_N|x_0,p_0,0) = &\sum_{n_N=-\infty}^{+\infty}\cdots\sum_{n_1=-\infty}^{+\infty}\int_0^{2\pi}\frac{dx_0}{2\pi}\delta(p-p_0) \\ &\times\int_0^{2\pi}dx_1\cdots\int_0^{2\pi}dx_{N-1}\delta(p_N-p_0 \\ &-S_{N-1})\delta(x_N-x_{N-1}-(t_N-t_N-1) \\ &\times[(p_{N-1}-KV'(x_{N-1}))] \\ &+2\pi n_N)\cdots\delta(p_1-p_0-S_0)\delta(x_1-x_0 \\ &-(t_1-t_0)[p_1-KV'(x_0)]+2\pi n_1). \end{aligned} \tag{A8}$$

Inserting the above equation into Eq. (A5) and taking into account the δ-function restraint on p_N, we find

$$\begin{aligned} D = &\frac{1}{2N}\sum_{n_N=-\infty}^{+\infty}\cdots\sum_{n_1=-\infty}^{+\infty}\prod_{i=0}^{N}\int_0^{2\pi}\frac{dx_i}{2\pi}S_N^2\delta(x_N-x_{N-1} \\ &-(t_N-t_N-1)(p_0+S_{N-1})+2\pi n_N)\cdots\delta(x_1-x_0 \\ &-(t_1-t_0)(p_0+S_0)+2\pi n_1). \end{aligned} \tag{A9}$$

By making use of the Poisson summation formula

$$\sum_{n=-\infty}^{+\infty}\delta(y+2\pi n) = \frac{1}{2\pi}\sum_{m=-\infty}^{+\infty}\exp[imy] \tag{A10}$$

we can write Eq. (A9) as

$$D = \frac{1}{2N}\sum_{m_N=-\infty}^{\infty}\cdots\sum_{m_1=-\infty}^{\infty}\prod_{i=0}^{N}\int_0^{2\pi}\frac{dx_i}{(2\pi)}S_N^2 \times\exp\left(\sum_{j=1}^{N}\{im_j[x_j-x_{j-1}-(t_j-t_{j-1})(p_0+S_{j-1})]\}\right). \tag{A11}$$

The term where $m_j=0$ for all j corresponds to the quasilinear diffusion

$$\begin{aligned} D &= \frac{1}{2N}\prod_{i=0}^{N}\int_0^{2\pi}\frac{dx_i}{(2\pi)}S_N^2 \\ &= \frac{1}{2N}\prod_{i=0}^{N}\int_0^{2\pi}\frac{dx_i}{(2\pi)}K^2[-V'(x_0)-V'(x_1)-\cdots V'(x_{N-1})]^2 \\ &= \frac{1}{2N}K_{\mathrm{eff}}^2\frac{N}{2} = \frac{K_{\mathrm{eff}}^2}{4}, \end{aligned} \tag{A12}$$

where we recall that $K_{\mathrm{eff}}=K\sqrt{1+4a^2}$.

All the other terms, where some of the m_j are nonzero, give corrections to this result. As noted in the text, the main corrections to the diffusion coefficient for the ratchet arise from correlations of the form $C(2,p)=\langle 2V'(x_j)V'(x_{j+2})\rangle$, obtained from Eq. (A11) by evaluating the contribution of $2V'(x_j)V'(x_{j+2})$ in the term S_N^2. The leading part of this contribution is obtained by setting $m_{j+2}=\pm 1$ and $m_{j+1}=-m_{j+2}$ (all other m are zero) for the $K\sin x$ part of the potential $V(x)$, and $m_{j+2}=\pm 2$ and $m_{j+1}=-m_{j+2}$ (all other m are zero) for the $Ka\sin 2x$ part of the potential $V(x)$ [12]. These corrections have to be summed over all kicks $j=1,\ldots,N$. Since there are three different time intervals between kicks ($T_1=1+b, T_2=1, T_3=1-b$), there are three different contributions to calculate. We now address individually each of these three contributions.

1. Correlation between kicks $i, i+2$

We choose the following map for this section:

$$\begin{aligned} x_i &= x_{i-1}+p_i(1+b), \\ x_{i+1} &= x_i+p_{i+1}, \\ x_{i+2} &= x_{i+1}+p_{i+2}(1-b), \\ p_i &= x_{i-1}-V'(x_{i-1}), \\ p_{i+1} &= x_i-V'(x_i), \\ p_{i+2} &= x_{i+1}-V'(x_{i+1}). \end{aligned} \tag{A13, A14}$$

We consider first the correction that arises as a result of the $K\sin x$ part of the potential. Setting $m_{i+2}=-1$ and $m_{i+1}=+1$ in Eq. (A11), and keeping the $2V'(x_{i+2})V'(x_i)$ term of S_N^2 we obtain

$$C(2,p)^{i:i+2}_{m_{i+2}=-1} = \frac{1}{2N}\prod_{j=0}^{N}\int_0^{2\pi}\frac{dx_j}{2\pi}2V'(x_{i+2})V'(x_i) \times e^{-i(x_{i+2}-x_{i+1}-(1-b)(p_0+S_{i+1}))} \times e^{+i(x_{i+1}-x_i-p_0-S_i)} = \frac{1}{N}\prod_{j=0}^{N}\int_0^{2\pi}\frac{dx_j}{2\pi}V'(x_{i+2})V'(x_i)e^{-i(x_{i+2}-2x_{i+1}+x_i)} \times e^{-ip_0b}e^{i((1-b)S_{i+1}-S_i)}. \quad \text{(A15)}$$

Now we use the fact that

$$S_{i+1}(1-b)+S_i = -(1-b)V'(x_{i+1}) - bS_i. \quad \text{(A16)}$$

Therefore the correction becomes

$$C(2,p)^{i:i+2}_{m_{i+2}=-1} = \frac{1}{N}\prod_{j=0}^{N}\int_0^{2\pi}\frac{dx_j}{2\pi}V'(x_{i+2})V'(x_i) \times e^{-i(x_{i+2}-2x_{i+1}+x_i)}e^{-ip_0b}e^{i(-(1-b)V'(x_{i+1})-bS_i)}. \quad \text{(A17)}$$

One can further simplify this equation by using the identity [$J_n(x)$ is the standard Bessel function]:

$$\exp[\pm iz\cos\theta] = \sum_n i^{\pm n}J_n(z)\exp[\pm in\theta] \quad \text{(A18)}$$

to obtain

$$C(2,p)^{i:i+2}_{m_{i+2}=-1} = \frac{1}{N}\prod_{j=0}^{N}\int_0^{2\pi}\frac{dx_j}{2\pi}V'(x_{i+2})V'(x_i)e^{-i(x_{i+2}-2x_{i+1}+x_i)} \times e^{-ip_0b}e^{-i\{(1-b)[K\cos(x_{i+1})+2Ka\cos(2x_{i+1})]+bS_i\}} = \frac{1}{N}\int_0^{2\pi}\frac{dx_j}{2\pi}V'(x_{i+2})V'(x_i)e^{-i(x_{i+2}-2x_{i+1}+x_i)} \times e^{-ip_0b}\sum_n i^{-n}J_n((1-b)K)e^{-inx_{i+1}} \times \sum_s i^{-s}J_s((1-b)2Ka)e^{-i2sx_{i+1}}e^{-ibS_i}. \quad \text{(A19)}$$

The integration over x_{i+1} gives

$$-nx_{i+1} - 2sx_{i+1} + 2x_{i+1} = 0 \Rightarrow n = 2-2s.$$

So, we finally obtain

$$C(2,p)^{i:i+2}_{m_{i+2}=-1} = \frac{1}{N}\prod_{j}\int_0^{2\pi}\frac{dx_j}{2\pi}V'(x_{i+2})V'(x_i)e^{-i(x_{i+2}+x_i)} \times e^{-ip_0b}\times\sum_s i^{-2+s}J_{2-2s}((1-b)K) \times J_s((1-b)2Ka)e^{-ibS_i}. \quad \text{(A20)}$$

The integrations over x_j with $j>i+2$ give simply 1. The integrations over x_j with $j<i$ are all identical. They give a contribution

$$[J_0(Kb)J_0(Kb2a)]^i. \quad \text{(A21)}$$

Since $Kb \ll 1$, $J_0(Kb)\simeq 1$, and one can neglect this term for short times (when the exponent i is not too large). We show, however, at the end of the Appendix that the longer time behavior (and so the ratchet time) can be obtained from this term. Finally, we are left with the integration over x_{i+2} and x_i. For the x_i part, it is easy to show that the term $\exp(-ibS_i)$ can be neglected for small b. The exponentials $\exp(-ix_{i+2}-ix_i)$ must be combined with the product $V'(x_{i+2})V'(x_i)$ to give a nonzero result. We expand the product in the following way:

$$V'(x_{i+2})V'(x_i) \equiv (K\cos x_{i+2} + 2Ka\cos 2x_{i+2}) \times (K\cos x_i + 2Ka\cos 2x_i) = K^2\cos x_{i+2}\cos x_i + 2K^2a\cos x_{i+2}\cos 2x_i + 2K^2a\cos 2x_{i+2}\cos x_i + 4(Ka)^2\cos 2x_{i+2}\cos 2x_i. \quad \text{(A22)}$$

The first term, which arises from the $K\sin x$ part of the potential, is here the appropriate one to use:

$$K^2\cos x_{i+2}\cos x_i = \frac{K^2}{4}\{e^{i(x_{i+2}-x_i)} + e^{-i(x_{i+2}-x_i)} + e^{i(x_{i+2}+x_i)} + e^{-i(x_{i+2}+x_i)}\}. \quad \text{(A23)}$$

The integrations are now trivial, and we get

$$C(2,p)^{i:i+2}_{m_{i+2}=-1} = \frac{K^2}{4N}e^{-ip_0b}\sum_s i^{-2+s}J_{2-2s}((1-b)K) \times J_2((1-b)2Ka). \quad \text{(A24)}$$

The same calculation for the case $m_{i+2}=1, m_{i+1}=-1$ simply gives the complex conjugate of this expression.

Combining these results, we get

$$C(2,p)^{i:i+2}_{K\sin x} = \frac{K^2}{4N}\sum_s J_{2-2s}((1-b)K)J_s((1-b)2Ka) \times\{i^{-2+s}e^{-ip_0b} + i^{2-s}e^{ip_0b}\} = -\frac{1}{2N}\sum_s J_{2-2s}((1-b)K)J_s((1-b)2Ka) \times\cos\left(p_0b - \frac{\pi}{2}s\right). \quad \text{(A25)}$$

Since we have $N/3$ terms of this kind [only for $1/3$ of the N kicks do we have the map chosen in this section, Eqs. (A13) and (A14)], we obtain the final form of the $i:i+2$ correction to the quasilinear diffusion resulting from the $K\sin x$ part of the potential as

$$C(2,p)^{i:i+2}_{K\sin x} = -\frac{K^2}{6}\sum_s J_{2-2s}((1-b)K)J_s((1-b)2Ka) \times\left(\cos p_0b\cos\frac{\pi}{2}s + \sin p_0b\sin\frac{\pi}{2}s\right). \quad \text{(A26)}$$

Taking now $m_{i+2}=\pm 2$ and $m_{i+1}=-m_{i+2}$ and following the same analysis we pick out the correction to the diffusion

coefficient due to the $Ka \sin 2x$ part of the potential, which is

$$C(2,p)^{i:i+2}_{Ka\sin 2x} = \frac{(2Ka)^2}{6}\sum_s J_{4-2s}(2(1-b)K)J_s(4(1-b)Ka) \times\left(\cos 2p_0 b\cos\frac{\pi}{2}s + \sin 2p_0 b\sin\frac{\pi}{2}s\right). \tag{A27}$$

2. Correlation between kicks $i+1, i+3$

The analysis for the correlation between kicks $i+1$ and $i+3$ of our cycle follows the same pattern as that given above, starting from the following three-kick map:

$$x_{i+1} = x_i + p_{i+1}, \tag{A28}$$

$$x_{i+2} = x_{i+1} + p_{i+2}(1-b), \tag{A29}$$

$$x_{i+3} = x_{i+2} + p_{i+3}(1+b), \tag{A30}$$

$$p_{i+1} = x_i - V'(x_i), \tag{A31}$$

$$p_{i+2} = x_{i+1} - V'(x_{i+1}), \tag{A32}$$

$$p_{i+3} = x_{i+2} - V'(x_{i+2}). \tag{A33}$$

One therefore obtains the diffusion correction due to $K \sin x$ for kicks $i+1:i+3$ to be

$$C(2,p)^{i+1:i+3}_{K\sin x} = -\frac{K^2}{6}\sum_s J_{2-2s}((1+b)K)J_s((1+b)2Ka) \times\left(\cos 2p_0 b\cos\frac{\pi}{2}s - \sin 2p_0 b\sin\frac{\pi}{2}s\right) \tag{A34}$$

with the $Ka \sin 2x$ correction being

$$C(2,p)^{i+1:i+3}_{Ka\sin 2x} = \frac{(2Ka)^2}{6}\sum_s J_{4-2s}(2(1+b)K)J_s(4(1+b)Ka) \times\left(\cos 4p_0 b\cos\frac{\pi}{2}s - \sin 4p_0 b\sin\frac{\pi}{2}s\right). \tag{A35}$$

Note that in this case we obtain correction terms that are dependent on $\sin 2pb$ and $\sin 4pb$, rather than $\sin pb$ and $\sin 2pb$ obtained from the $i:i+2$ correlation.

3. Correlation between kicks $i+2, i+4$

Once again, we begin by defining the map

$$x_{i+2} = x_{i+1} + p_{i+2}(1-b), \tag{A36}$$

$$x_{i+3} = x_{i+2} + p_{i+3}(1+b), \tag{A37}$$

$$x_{i+4} = x_{i+3} + p_{i+4}, \tag{A38}$$

$$p_{i+2} = x_{i+1} - V'(x_{i+1}), \tag{A39}$$

$$p_{i+3} = x_{i+2} - V'(x_{i+2}), \tag{A40}$$

$$p_{i+4} = x_{i+3} - V'(x_{i+3}). \tag{A41}$$

The analysis then follows precisely the same procedure given above, resulting in the $K \sin x$ correction

$$C(2,p)^{i+2:i+4}_{K\sin x} = -\frac{K^2}{6}\sum_s J_{2-2s}(K)J_s(2Ka) \times\left(\cos p_0 b\cos\frac{\pi}{2}s + \sin p_0 b\sin\frac{\pi}{2}s\right) \tag{A42}$$

and the $Ka \sin 2x$ correction

$$C(2,p)^{i+2:i+4}_{Ka\sin 2x} = \frac{(2Ka)^2}{6}\sum_s J_{4-2s}(2K)J_s(4Ka) \times\left(\cos 2p_0 b\cos\frac{\pi}{2}s + \sin 2p_0 b\sin\frac{\pi}{2}s\right). \tag{A43}$$

4. Total correction from the two-kick correlation

Combining these contributions together one obtains

$$\begin{aligned} C(2,p) = \frac{1}{6}\Bigg[& K^2\sum_s J_{2-2s}((1-b)K)J_s((1-b)2Ka) \\ & \times\left(\cos p_0 b\cos\frac{\pi}{2}s + \sin p_0 b\sin\frac{\pi}{2}s\right) \\ & + (2Ka)^2\sum_s J_{4-2s}(2(1-b)K)J_s(4(1-b)Ka) \\ & \times\left(\cos 2p_0 b\cos\frac{\pi}{2}s + \sin 2p_0 b\sin\frac{\pi}{2}s\right) \\ & - K^2\sum_s J_{2-2s}((1+b)K)J_s((1+b)2Ka) \\ & \times\left(\cos 2p_0 b\cos\frac{\pi}{2}s - \sin 2p_0 b\sin\frac{\pi}{2}s\right) \\ & + (2Ka)^2\sum_s J_{4-2s}(2(1+b)K)J_s(4(1+b)Ka) \\ & \times\left(\cos 4p_0 b\cos\frac{\pi}{2}s - \sin 4p_0 b\sin\frac{\pi}{2}s\right) \\ & - K^2\sum_s J_{2-2s}(K)J_s(2Ka)\left(\cos p_0 b\cos\frac{\pi}{2}s \right. \\ & \left. + \sin p_0 b\sin\frac{\pi}{2}s\right) + (2Ka)^2\sum_s J_{4-2s}(2K)J_s(4Ka) \\ & \times\left(\cos 2p_0 b\cos\frac{\pi}{2}s + \sin 2p_0 b\sin\frac{\pi}{2}s\right)\Bigg]. \end{aligned}$$

As the build up of asymmetry in the system is a short-time effect, we can neglect any terms that are symmetric with respect to momentum over this period. We therefore attribute the onset of transport solely to the sin pb dependent terms in the diffusion coefficient. We therefore simplify Eq. (3.6) to

$$\begin{aligned}C(2,p)_{\text{asymm}} = \frac{K^2}{6}\Bigg(&- \sum_s J_{2-2s}((1-b)K)J_s((1-b)2Ka)\\ &\times \sin p_0 b \sin\frac{\pi}{2}s + (2a)^2\sum_s J_{4-2s}(2(1-b)K)\\ &\times J_s(4(1-b)Ka)\sin 2p_0 b \sin\frac{\pi}{2}s + \sum_s J_{2-2s}((1\\ &+ b)K)J_s((1+b)2Ka)\\ &\times \sin 2p_0 b \sin\frac{\pi}{2}s - (2a)^2\sum_s J_{4-2s}(2(1+b)K)\\ &\times J_s(4(1+b)Ka)\sin 4p_0 b \sin\frac{\pi}{2}\\ &- \sum_s J_{2-2s}(K)J_s(2Ka)\sin p_0 b \sin\frac{\pi}{2}s\\ &+ (2a)^2\sum_s J_{4-2s}(2K)J_s(4Ka)\sin 2p_0 b \sin\frac{\pi}{2}s\Bigg).\end{aligned} \tag{A44}$$

These formulas can now be rearranged to give the total correction to the diffusion coefficient as a function of the three sin npb present (note that we use $s'=2-2s$ and $s''=4-2s$ for clarity):

$$\begin{aligned}C(2,p)_{\text{asymm}} = -\frac{K^2}{6}\Bigg[&\sin p_0 b\Bigg\{\sum_s [J_{s'}(K)J_s(2Ka)\\ &+ J_{s'}(K(1-b))\\ &\times J_s(2Ka(1-b))]\sin\frac{\pi}{2}s\Bigg\}\\ &- \sin 2p_0 b\Bigg\{(2a)^2\sum_s [J_{s''}(2K)J_s(4Ka)\\ &+ J_{s'}(K(1+b))J_s(2Ka(1+b))\\ &+ (2a)^2 J_{s''}(2K(1-b))J_s(4Ka(1-b))]\sin\frac{\pi}{2}s\Bigg\}\\ &+ \sin 4p_0 b\Bigg\{(2a)^2\sum_s J_{s''}(2K(1+b))\\ &\times J_s(4Ka(1+b))\sin\frac{\pi}{2}s\Bigg\}\Bigg].\end{aligned} \tag{A45}$$

5. Derivation of ratchet time t_r

We now come back to the time dependence of the corrections to the diffusion coefficient, to calculate the ratchet time. When calculating the corrections coming from the $(i,i+2)$ correlations, we have neglected terms such as

$$[J_0(Kb)J_0(Kb2a)]^k. \tag{A46}$$

In Eq. (A25) if we included these terms we would have

$$\begin{aligned}C(2,p)^{i:i+2}_{K\sin x} = &-\frac{1}{4N}\sum_s J_{2-2s}((1-b)K)J_s((1-b)2Ka)\\ &\times\cos\left(p_0 b - \frac{\pi}{2}s\right)\sum_{k=1}^{k=N/3}(J_0(Kb)J_0(Kb2a))^k.\end{aligned} \tag{A47}$$

In the previous sections we assumed $J_0(Kb)\simeq J_0(Kb2a)\simeq 1$ so the sum over k simply yielded a factor of $N/3$. Although $J_0(Kb)\simeq 1-(Kb)^2/4$ is very close to 1, when the number of kicks (and so, i) increases, this term becomes eventually much smaller than 1. The sum cannot then simply be equated to $N/3$. We must sum between kicks N and kick 1 (with only 1 kick over 3 contributing to this correction)

$$\begin{aligned}&[J_0(Kb)J_0(Kb2a)]^N + [J_0(Kb)J_0(Kb2a)]^{N-3}\\ &+ [J_0(Kb)J_0(Kb2a)]^{N-6} + \cdots.\end{aligned} \tag{A48}$$

This is just a geometrical series, summing up to

$$\frac{1-[J_0(Kb)J_0(Kb2a)]^N}{1-[J_0(Kb)J_0(Kb2a)]^3}. \tag{A49}$$

As a function of the kick number N, this increases linearly for small N (and thus gives a correction to the diffusion coefficient), but saturates for large N at the value $\{1-[J_0(Kb)J_0(Kb2a)]^3\}^{-1}$ (where the diffusion coefficient is not affected by these correlations anymore). Note that for the sin $2pb$ and sin $4pb$ terms the Bessel functions have arguments two or four times larger respectively. Hence in the main paper we introduce the time dependence function

$$\Phi(N,bK,n) = \frac{3}{N}\frac{1-[J_0(nbK)J_0(2nabK)]^{N-1}}{1-[J_0(bK)J_0(2nabK)]^3}. \tag{A50}$$

This multiplies the diffusion rates $C(2,p)$ which were obtained with the approximation $[J_0(Kb)J_0(Kb2a)]^k\simeq 1$.

We define the ratchet time t_r as the time needed for the function $\Phi(N,b,n)N$ to attain 95% of its saturated value as $N\to\infty$. This gives

$$t_r \simeq \frac{\ln(5/100)}{\ln[J_0(bK)J_0(2abK)]}. \tag{A51}$$

Keeping only the lowest order in b, we get

$$t_r = \frac{4\ln(20)}{b^2K_{\text{eff}}^2}, \tag{A52}$$

where we recall $K_{\mathrm{eff}}^2 = K^2(1+4a^2)$. Note that this is the ratchet time for the dominant $\sin pb$ contribution to the diffusion coefficient. One can calculate in the same way the ratchet times for the $\sin 2pb$ and $\sin 4pb$ contributions. For $a = 1/2$ we get

$$t_r^{(\sin pb)} = \frac{2\ln(20)}{(Kb)^2}, \tag{A53}$$

$$t_r^{(\sin 2pb)} = \frac{2\ln(20)}{(2Kb)^2}, \tag{A54}$$

$$t_r^{(\sin 4pb)} = \frac{2\ln(20)}{(4Kb)^2}. \tag{A55}$$

[1] G. Casati, B. V. Chirikov, F. M. Izraelev, and J. Ford, in *Lecture notes in Physics* (Springer, Berlin, 1979), Vol. 93, p. 334.

[2] S. Fishman, D. R. Grempel, and R. E. Prange, Phys. Rev. Lett. **49**, 509 (1982).

[3] F. L. Moore, J. C. Robinson, C. F. Bharucha, Bala Sundaram, and M. G. Raizen, Phys. Rev. Lett. **75**, 4598 (1995).

[4] P. Reimann, Phys. Rep. **361**, 57 (2002).

[5] S. Flach, O. Yevtushenko, and Y. Zolotaryuk, Phys. Rev. Lett. **84**, 2358 (2000); S. Denisov, S. Flach, A. A. Ovchinnikov, O. Yevtushenko, and Y. Zolotaryuk, Phys. Rev. E **66**, 041104 (2002).

[6] T. Dittrich, R. Ketzmerick, M.-F. Otto, and H. Schanz, Ann. Phys. (Leipzig) **9**, 1 (2000); H. Schanz, M.-F. Otto, R. Ketzmerick, and T. Dittrich, Phys. Rev. Lett. **87**, 070601 (2001).

[7] T. S. Monteiro, P. A. Dando, N. A. C. Hutchings, and M. R. Isherwood, Phys. Rev. Lett. **89**, 194102 (2002).

[8] T. Jonckheere, M. R. Isherwood, and T. S. Monteiro, Phys. Rev. Lett. **91**, 253003 (2003).

[9] P. H. Jones, M. Goonasekera, H. E. Saunders-Singer, and D. Meacher, e-print quant-ph/0309149.

[10] A. J. Lichtenberg and M. A. Lieberman, *Regular and Chaotic Dynamics* (Springer-Verlag, New York, 1992).

[11] D. L. Shepelyansky, Phys. Rev. Lett. **56**, 677 (1986).

[12] A. B. Rechester and R. B. White, Phys. Rev. Lett. **44**, 1586 (1980).

[13] Matthew Isherwood, Ph.D. thesis, http://www.tampa.phys.ucl.ac.uk/ UCL, 2004.